Heat capacities of helium in one- and three-dimensional channels at low temperatures



1993 J. Phys.: Condens. Matter 5 1619

(http://iopscience.iop.org/0953-8984/5/11/003)

J. Phys.: Condens. Matter 5 (1993) 1619–1632. Printed in the UK

# Heat capacities of helium in one- and three-dimensional channels at low temperatures

Kensuke Konishi, Hiroyuki Deguchi and Kazuyoshi Takeda
Department of Applied Science, Faculty of Engineering, Kyusyu University, Fukuoka 812, Japan

Received 17 November 1992, in final form 4 January 1993

**Abstract.** The heat capacities of $^4$He and $^3$He atoms adsorbed in porous high-silica zeolites having channels about 5.5 Å in diameter have been measured below 6 K. In neither atom is the expected quantum degeneracy detected. In one-dimensional channels, in which the direct positional exchange of atoms is prohibited, the heat capacity depends linearly on temperature, $T$, as $C = AT$. This result can be understood by the tunnelling two-level system model for glasses or amorphous solids at very low temperatures. The large zero-point motion of the helium atom is reflected in the enormous value of the coefficient $A$, and in the wider temperature range of the linear term than in glasses. In three-dimensional channels, the heat capacity of helium atoms shows a shoulder around 2 K for lower atomic concentrations. The result below 2 K is reproduced by a consideration of discrete energy levels enhanced in the crossing space of channels. For higher concentrations the heat capacity shows a linear temperature dependence, which can be understood using the same picture as in the case of the one-dimensional system.

## 1. Introduction

In recent years, investigation of quantum fluids such as $^4$He and $^3$He in certain restricted geometries has been a fundamental problem in the study of possible quantum degeneracy. In most experimental work carried out to date, the restriction has been performed by the use of substrates such as Vycor glass [1–4], grafoil [5], zeolite [6–9], and so on. In the case of zeolite and Vycor glass, the average pore size ranges from 10 Å to $10^4$ Å. The restriction in these substrates is not so severe as to preclude the positional exchange of any two atoms in space, and various evidence relating to quantum degeneracy has been reported.

However, it is interesting and important to see whether quantum degeneracy can occur in a more restricted space, where atoms cannot directly exchange their position. The superfluid transition of $^4$He is suggested on theoretical grounds to occur in a zeolite, which has small channels with a size comparable to a helium atom [10–12]. Experimentally, the Fermi degeneracy of $^3$He in one-dimensional channels of size 5.5 Å has been studied, where the susceptibility of $^3$He obeys the Curie law down to 0.1 K without giving the Pauli paramagnetic behaviour that characterizes Fermi statistics. In other zeolites, where the positional exchange of $^3$He atoms may be possible, the susceptibility shows the Pauli paramagnetic behaviour, suggesting the occurrence of the Fermi degeneracy [13]. However, the thermal behaviour of $^3$He in such a severely restricted geometry is not clear, nor is the quantum degeneracy

0953-8984/93/111619+14$07.50  

of $^4$He. In this paper, we study the thermal behaviour of these atoms in one- and three-dimensional channels using high-silica zeolites. The advantage of using these zeolites is their electrical neutrality, which is an inevitable experimental requirement, as will be emphasized in section 2. Using various zeolites, having a larger pore size and cations on the framework, a series of pioneer works on quantum particles has been carried out by Wada, Watanabe and co-workers. Their results will be given in section 3, in comparison with our present results.

## 2. Experimental techniques

For the present study of helium, it is necessary to prepare restricted channels electrically free from cations or anions on their framework; helium atoms in channels with some electric polarization are likely to be bound or trapped around them [8,9]. Here, we use two high-silica zeolites: $Na_nAl_nSi_{24-n}O_{48}$ (hereafter called ZSM-23 ($n = 0.738$)) with lattice parameters $a = 5.2$ Å, $b = 21.5$ Å, $c = 11.1$ Å for the unit cell [14], and $Na_nAl_nSi_{96-n}O_{192}$ (ZSM-5 ($n = 0.101$)) with $a = 20.1$ Å, $b = 19.9$ Å, $c = 13.4$ Å [15–17]. The channel structure of these zeolites is shown in figure 1. The zeolite ZSM-23 has one-dimensional channels parallel to [100] enclosed by a ten-membered atomic ring of size 5.3 Å × 5.6 Å. The porosity is 0.21 cm$^3$ g$^{-1}$. The zeolite ZSM-5, however, has a three-dimensional network of channels enclosed with ten-membered atoms. Straight channels parallel to [010] have openings of size 5.4 Å × 5.6 Å, and zigzag channels along [100] have openings of size 5.1 Å × 5.7 Å. The porosity of ZSM-5 is 0.32 cm$^3$ g$^{-1}$. In ZSM-23, the direct positional exchange of helium atoms is prohibited within a channel. In ZSM-5, however, the exchange is possible through three-dimensional paths. Another profitable feature of these zeolites is the high value of the $SiO_2/Al_2O_3$ ratio, which is a measure of electrical neutrality on the framework; the ratio for ZSM-23 is 63 and that for ZSM-5 is 1900. Zeolites that have a ratio larger than $5 \sim 10$ are usually referred to as 'high-silica' zeolites.

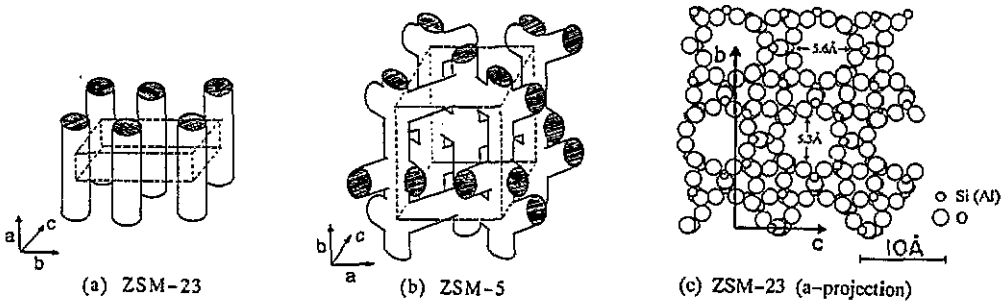


**Figure 1.** Channel structure of (*a*) ZSM-23 and (*b*) ZSM-5. The broken lines indicate the unit cell employed in this paper. (*c*) The framework of ZSM-23 (*a* projection).

The high-silica zeolites used here are powdered specimens with an average size of about 1 $\mu$m. Dehydration of these specimens is carried out by keeping them at a temperature around 500 °C for five hours. After dehydration, each specimen is packed in a copper cell for the heat capacity measurements. The sample cell is set to a $^3$He cryostat, and connected to a gas-handling system through a small capillary for the

introduction of He gas, as shown in figure 2. Before the introduction of the sample gas, final dehydration is performed at 220 °C for several hours in a high-vacuum atmosphere. A sample of $^3$He or $^4$He gas is then let into the cell and adsorbed in the temperature range between 77 K and 4.2 K. After annealing the sample system up to a temperature above 5 K and cooling to 0.8 K, the measurement of heat capacities of He adsorbed in high-silica zeolites is performed using the conventional adiabatic DC pulse method until about 6 K, at which temperature the He atoms begin to escape from the channels in the zeolite.

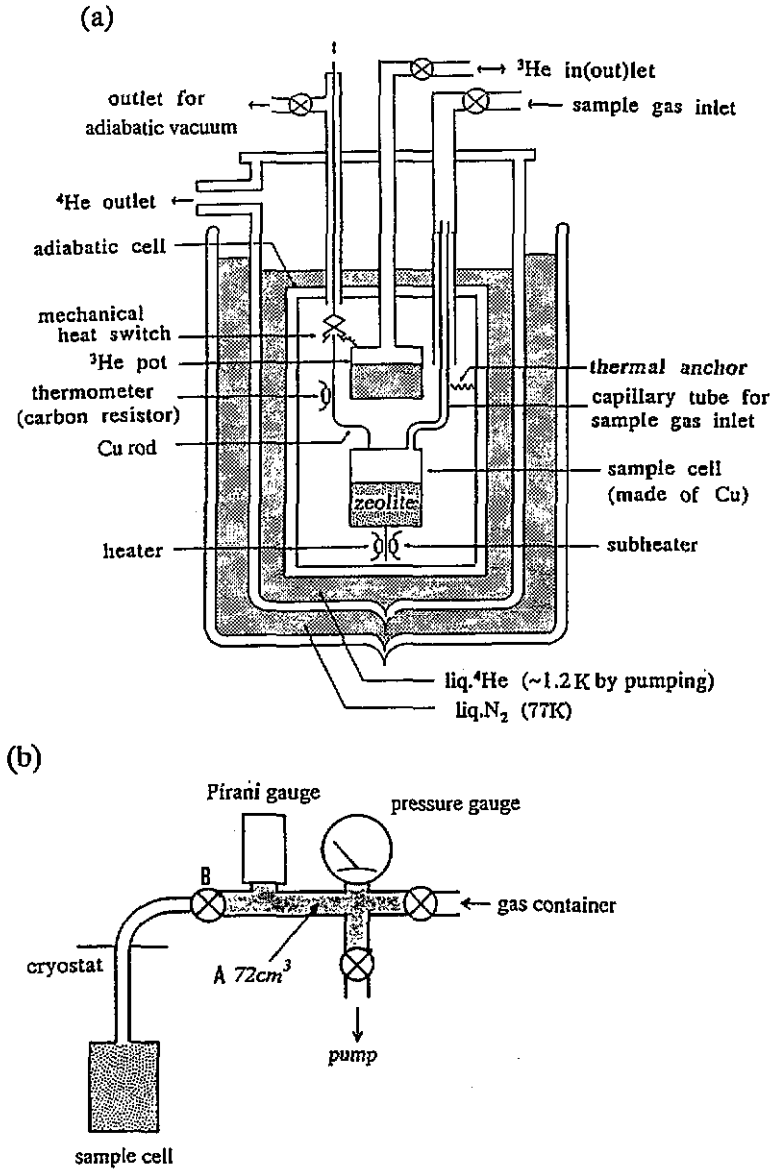


**Figure 2.** Schematic diagram of the cryostat (*a*) and the gas-handling system (*b*).

## 3. Results and Discussion

### *3.1. Adsorption isotherms of the zeolites*

First, we estimate the effective porosity volume in zeolites by the maximum number of helium atoms to be contained, assuming that helium atoms are free particles with a diameter of about 3 Å and assuming that the surfaces of the channels are flat. In the case of one-dimensional channels in ZSM-23, nearly 3.5 atoms are allowed to be contained in a unit cell, as shown in figure 3(*a*)-1. The restricted space in ZSM-5 is realized by the repetition of cages with four open channels, as in figures 3(*b*) and 1(*b*). The maximum number of atoms is expected to be about 11 for one cage with a structure as illustrated in the figure.

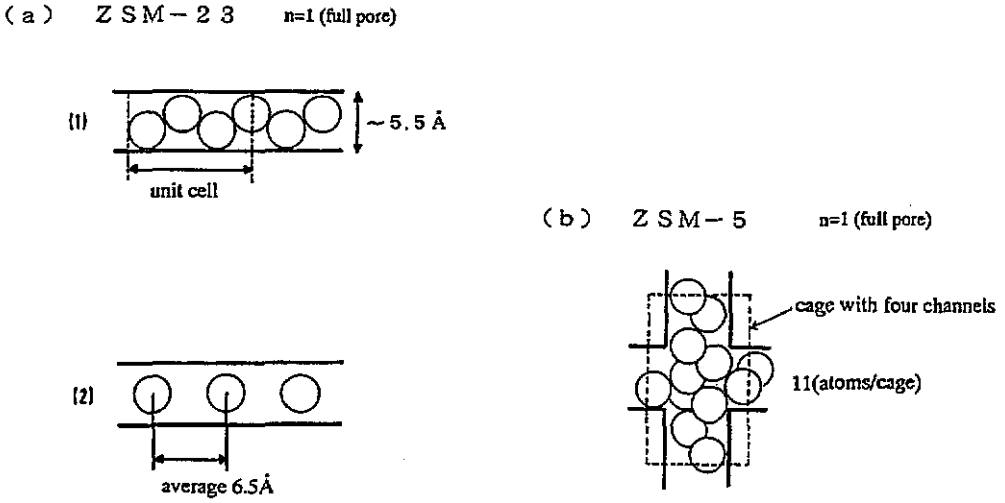


**Figure 3.** Schematic illustration for fully filled He atoms. (*a*) 1: hard-sphere particles fully packed in ZSM-23. 2: expected average arrangement of He atoms in ZSM-23 at $N_c$. (*b*) Expected average arrangement of He atoms in ZSM-5 at $N_c$. The broken lines indicate a cage with four open channels. Four cages are included in a unit cell.

In order to check whether the maximum volume mentioned above is really the case, we checked the dependence of the isothermal pressure on the concentration of adsorbate gases. A known amount of gas was prepared in the space A (see figure 2(*b*)) with a volume of 72 $cm^3$. After the gas was introduced into the sample cell through the valve B, the gas pressure was measured at room temperature with a Pirani gauge, once sufficient time had elapsed for the pressure to reach equilibrium. It is expected that, for a small amount of gas, most molecules will be adsorbed within the channels and the pressure will be small. In accordance with the increase of the amount of gas to fill the channels of the zeolite, at a certain concentration the pressure is expected to increase abruptly.

The experimental results are shown in figures 4(*a*) and (*b*) for ZSM-23 and ZSM-5, respectively. The data for $^4He$ and $^3He$ were taken at 4.2 K, and those for Ne at 27 K. The data for $N_2$, as in figure 4(*b*), were obtained at 77 K. In all cases, the pressure maintains a nearly constant value until the gas concentration reaches a critical value,

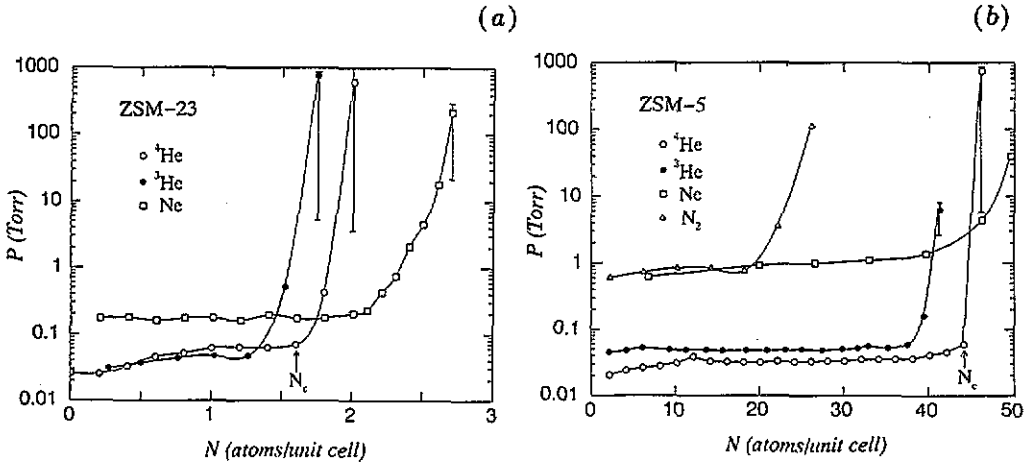


**Figure 4.** Adsorption isotherms of $^3$He, $^4$He (at 4.2 K), Ne (at 27 K) and $N_2$ (at 77 K) in (*a*) ZSM-23 and (*b*) ZSM-5. The full curves are to guide the eye.

$N_c$, above which the pressure increases abruptly. For concentrations lower than $N_c$, the pressure is small compared to the background pressure in the gas-handling system. In this concentration region, the value of the pressure for $^4$He and $^3$He is nearly the same, and smaller than that of $N_2$ by one order of magnitude. This is due to the difference of the background pressure at 4.2 K and 77 K.

The critical value, $N_c$, for He is about two times larger than that for $N_2$, and the critical value for $^4$He is slightly larger than that for $^3$He. In the case of ZSM-23, the critical value for $^4$He is determined, from figure 4, to be 1.6 atoms per unit cell. This concentration gives an average interatomic distance of 6.5 Å in channels. Similarly, in the case of ZSM-5, the critical value for $^4$He is determined to be 44 atoms per unit cell (11 atoms per cage). The value of $N_c$ for $N_2$ is about 20 molecules per unit cell, which is consistent with the value reported in [17]. The observed value of $N_c = 1.6$ atoms per unit cell for $^4$He, for ZSM-23 with one-dimensional channels, is rather smaller than the maximum value of 3.5 atoms per unit cell estimated geometrically at the beginning of this section. This may be responsible for the enhanced zero-point motion of particles in narrow channels. We can demonstrate the effect of the zero-point motion of helium atoms by substituting them with neon atoms, which are more hard sphere like, are without quantum effects and are very closely packed, giving much of the value of $N_c$, as in figure 4.

Hereinafter, we define the concentration $n$ of helium atoms in the zeolite to be the ratio of the number, $N$, of adsorbed atoms to the critical value $N_c$: $n = N/N_c$.

### *3.2. He in ZSM-23 (one-dimensional system)*

Measurements of heat capacity have been carried out for various concentrations of $^3$He and $^4$He adsorbed in ZSM-23. The results for $^4$He are shown in figure 5(*a*). The heat capacities of the zeolite itself are subtracted here. The dotted curve shows the heat capacity for liquid $^4$He. In the present data, no trace of the superfluid transition can be seen. Since the surface area of ZSM-23 is not negligible, it is expected that the atoms of helium are likely to become adsorbed on the surface of the specimen and form a two-dimensional solid at low temperatures. The low-temperature heat capacities of the two-dimensional solids of $^4$He and $^3$He are known

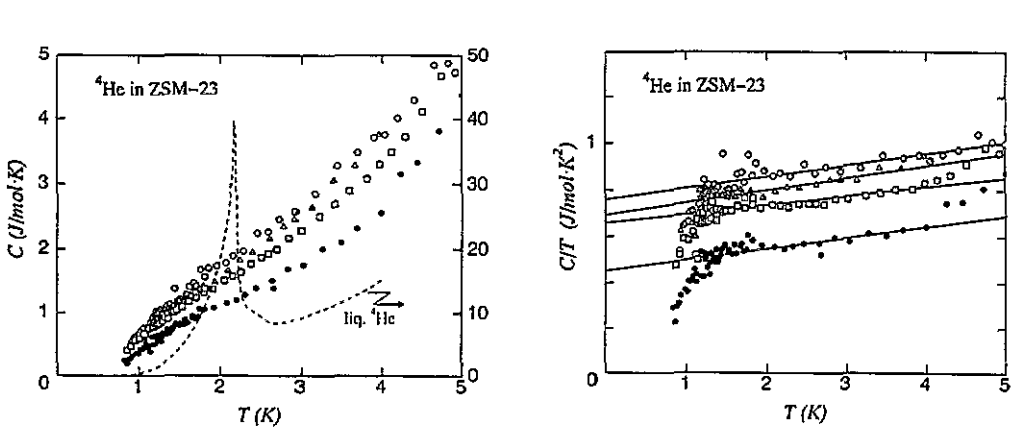


**Figure 5.** (*a*) Molar heat capacities of $^4$He in ZSM-23. (*b*) Plot of $C/T$ against $T$. The data points o, △, □ and • correspond to the amount of adsorbed $^4$He in the zeolite (1 g), respectively 0.58, 0.88, 1.34 and 1.81 mmol.

to show a $b(\theta_{2d})T^2$ dependence, where $\theta_{2d}$ is the characteristic two-dimensional Debye temperature. In order to check the contribution from the surface, in figure 5(*b*) we plot the data of the heat capacity $C$ of $^4$He adsorbed in ZSM-23 for $C/T$ against $T$. The data can be reproduced by $C = aT + bT^2$ above 1.3 K. In the case of $^4$He, the coefficient $a$ decreases with increasing concentration, and the coefficient $b$ is nearly constant. The $T^2$ contribution may be understood as being due to the two-dimensional $^4$He solid adsorbed on the surface of the specimen, as mentioned above.

In order to extract the intrinsic thermal behaviour of helium in the one-dimensional channel, we subtract the contribution $bT^2$. From this value of $b$, we can estimate the number of helium atoms on the surface using the known value of the two-dimensional Debye temperatures, 38 K and 32 K for $^3$He and $^4$He, respectively, which are the most profitable values for the two-dimensional helium solid [18]. Figure 6(*a*) shows the heat capacity of $^4$He without the contribution from $bT^2$, where the value of the heat capacity is renormalized for the helium atoms in the one-dimensional channels. It should be noted here that the heat capacity reveals the characteristic linear dependence $C = A(n)T$ above 1.3 K.

In the case of $^3$He, similar results are obtained by subtracting the contribution $bT^2$, as shown in figure 6(*b*). Below 1.3 K, heat capacities become smaller than $A(n)T$. The coefficient $A(n)$ decreases with increasing concentration $n$ for both $^3$He and $^4$He, as shown in figure 7.

Here, we consider the linear dependence of the heat capacity. There are two possible explanations for the origin of the linear contribution of $A(n)T$ in the one-dimensional channels. The first is due to the one-dimensionality of solid helium, and the second is due to the semi-quantum liquid state [19].

For the one-dimensional solid model, at low temperatures $C$ is expressed as

$$C = \tfrac{1}{3}\pi^2 R(T/\theta_{1d}) \tag{1}$$

where $R$ is the gas constant and $\theta_{1d}$ is the Debye temperature for the one-dimensional solid. When we equate (1) to the observed value of $A(n)T$, the Debye temperature

(*a*) (*b*)

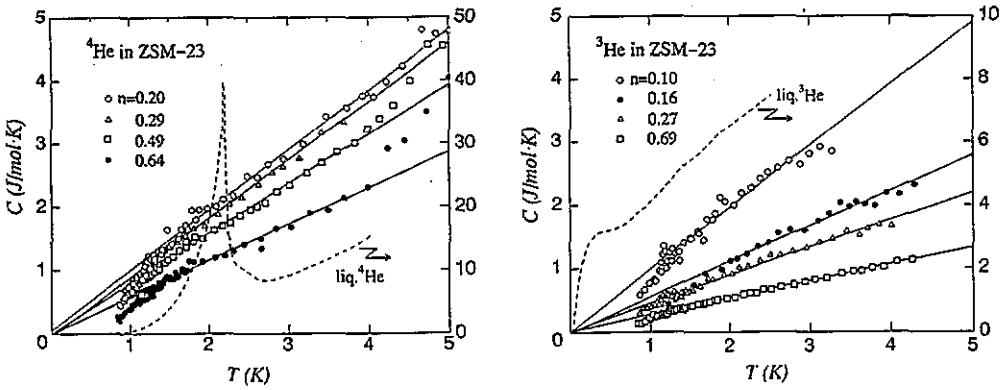


**Figure 6.** Heat capacities of He in ZSM-23 after subtraction of the surface effect. (*a*) $^4$He. $n = 0.20$ (o), 0.29 (△), 0.49 (□) and 0.64 (•). The broken curve shows the heat capacity of liquid $^4$He. (*b*) $^3$He. $n = 0.10$ (o), 0.16 (•), 0.27 (△) and 0.69 (□). The broken curve shows the heat capacity of liquid $^3$He. The full lines are to guide the eye.

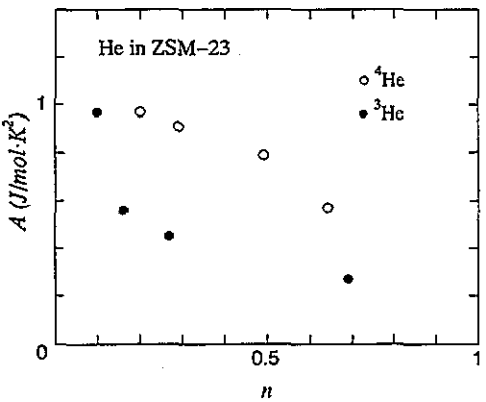


**Figure 7.** Concentration dependence of the coefficient $A(n)$ for $^4$He (o) and $^3$He (•) in ZSM-23.

$\theta_{1d}$ can be expressed in terms of the observed value of $A(n)$:

$$\theta_{1d} = \pi^2 R/3A(n). \tag{2}$$

The value of $\theta_{1d}$ for $^4$He varies considerably, from 28 K to 48 K, as the concentration changes from $n = 0.20$ to $n = 0.64$. For $^3$He, $\theta_{1d}$ ranges between 28 K and 102 K for the concentration range between $n = 0.10$ and $n = 0.69$. Generally, the Debye temperature should be independent of the concentration or cluster size, except in the case where the softening of phonons has an effect [20]. Therefore, the present analysis of the one-dimensional solid model is not reasonable.

A second possible explanation for the linear heat capacity is the effect of the irregular configuration of helium atoms in the channels. It is well known that the heat capacity of an irregular system or glassy state depends linearly on $T$ at low

temperatures. The thermal properties of glasses were explained in the tunnelling two-level system by Anderson and co-workers [21] and Phillips [22]. In this model, the atoms can sit around individual local minima formed by their own random configuration, and transfer among the minima by tunnelling. Single tunnelling occurs between neighbouring asymmetric wells. When the energy difference of the two wells is $\epsilon$, the free energy for single tunnelling is expressed as

$$f(\epsilon) = -k_B T \log(1 + e^{-\epsilon/k_B T}) \tag{3}$$

where $k_B$ is the Boltzmann constant. The free energy for independent tunnelling among all the possible potential levels is

$$F = -k_B T \int_0^\infty \nu \log(1 + e^{-\epsilon/k_B T})\, d\epsilon \tag{4}$$

where $\nu$ is the density of states. Assuming that $\nu$ does not depend on the energy difference in the glassy state at low temperatures [21,22], the heat capacity becomes

$$C = \tfrac{1}{6}\pi^2 \nu R T \equiv AT. \tag{5}$$

In real glass materials, the linear term is observed below 1 K (i.e. $T/\theta_D < 0.01$), and amounts to roughly $10^{-5}T \sim 10^{-4}T$ J mol$^{-1}$ K$^{-1}$, where $\theta_D$ is the Debye temperature [23].

There are a few points to stress about our present results when compared with the case for glasses. The first point is that the absolute value of the coefficient $A$ is 4~5 orders of magnitude larger than that for glasses. Another point is that the temperature range over which the heat capacity preserves the linear dependence is much wider for helium than for glasses. The linearity is observed below 4 K ($T/\theta_D < 0.13$) in helium and below 1 K ($T/\theta_D < 0.01$) in glasses. The coefficient $A(n)$ is related to the density of states, $\nu$, as described in (5). In the above model, $\nu$ is assumed to be independent of energy at low temperatures [20] and to be a function of $z/U$, where $U$ is the potential barrier and $z$ is the number of vacant neighbouring positions [19]. However, the value of $A$ should depend on the probability of the tunnelling, though this is not explicitly expressed in the above model for the heat capacity. The probability in helium is much larger than in glasses, because the potential barrier of helium is $U \simeq 10$ K and that of glasses is $U \simeq 10^3$ K. Moreover the tunnelling is assisted by strong zero-point motion in the case of helium. These characteristic features of helium are mainly responsible for the difference in the low-temperature heat capacities between helium and glasses.

In the case of helium, as shown in table 1, the coefficient $A$ seems to depend upon the topological configuration of the helium atoms: the values for helium in zeolites are smaller than those for liquid helium under pressure [19]. The values of $A(n)$ for the present one-dimensional channel give the smallest values in other cases. The Y zeolite has a three-dimensional channel structure whose channel and cage size are nearly 8 Å and 13 Å, respectively. The L zeolite has a one-dimensional channel structure whose size is almost the same as for the Y zeolite. In the table we can see that $A(n)$ decreases as the dimensionality and the pore size in the zeolites decreases.

Here, we consider the concentration dependence of $A(n)$. The value of $A(n)$ decreases with increasing concentration, as shown in figure 7, though the decrease is

**Table 1.** A comparison of $A(n)$ and the temperature range $(T/\theta_D)$ obtained for several systems.

| System | Pore size (Å) | $A(n)$ ($J\,mol^{-1}\,K^{-1}$) | Temperature range (K) $(T/\theta_D)$† | Ref. |
|---|---|---|---|---|
| Bulk $^4He$ | — | 2.3 | $1.9 \sim 9.2$ $(0.06 \sim 0.3)$ | [19] |
| Bulk $^3He$ | — | 3.9 | $0.8 \sim 1.9$ $(0.06 \sim 0.14)$ | [19] |
| $^4He$ in Na-Y zeolite | 8, 13 (3D) | 2.2 | — | [6] |
| $^4He$, $^3He$ in K-L zeolite | 7.4, 13 (1D) | ~1.0 | — | [9] |
| $^4He$ in ZSM-23 | 5.5 (1D) | $0.57 \sim 0.97$ | $1.3 \sim 4$ $(0.04 \sim 0.13)$ | ‡ |
| $^3He$ in ZSM-23 | 5.5 (1D) | $0.27 \sim 0.97$ | $1.3 \sim 4$ $(0.04 \sim 0.13)$ | ‡ |
| Glass $SiO_2$ | — | $6.0 \times 10^{-5}$ | <1 (< 0.01) | [23] |
| Glass $GeO_2$ | — | $1.6 \times 10^{-4}$ | <1 (< 0.01) | [23] |
| Glass Se | — | $5.5 \times 10^{-5}$ | <1 (< 0.01) | [23] |

† The Debye temperature for helium in zeolite and glass is assumed to be about 30 K and 100 K, respectively.
‡ Present work.

not systematic. We can qualitatively understand this decrease in $A(n)$ as being due to the reduction in the number of vacant sites with increasing concentration.

Furthermore, we discuss here the difference between the present linear dependence of the heat capacity in a restricted geometry, and that of liquid helium under pressure, as obtained by Andreev [19]. In the latter case, the linear dependence was obtained under a pressure of 25 atm and in a temperature region $0.06\theta_D < T < 0.3\theta_D$, where $\theta_D$ is the Debye temperature of $^4He$ in the liquid state. In other words, it is the effect of pressure that restricts the positional exchange of helium atoms and gives a linear heat capacity. Contrary to this case, our present results reveal that a restriction of topological space, in which the positional exchange of the particles is impossible, also gives semi-quantum behaviour, such as a linear heat capacity.

In order to demonstrate the semi-quantum behaviour as observed in the present system, we measured the heat capacity of neon adsorbed in the same zeolite. Our preliminary results show no evidence of a linear dependence of the heat capacity above 2 K. We can understand this by taking into consideration that the quantum parameter is much smaller for neon than helium. The results are to be given elsewhere.

In the above model, we have treated helium atoms in the present high-silica zeolite as quantum particles without being trapped on the framework atoms of the channels. However, is this really the case? There are several theoretical works relating to this problem. The potential of a particle restricted in a cylindrical micropore is estimated as a function of the diameter of the cylinder, which gives its minimum at the centre of the cylinder when the diameter of the cylinder is smaller than twice the particle size [24]. On the other hand, the interaction between particles in the comparable size of channels is found to be much weaker than in free space [25]. In the real case of the Y and L zeolites, which have a larger pore size than the present case and have cations on the inside wall, a certain number of adsorbed atoms are shown to be trapped on the cations, and the rest behave like a semi-quantum liquid [6,9].

We now return to the present results at the lowest temperatures (figure 6). Below 1.3 K the heat capacity does not depend linearly on temperature. There is no heat

capacity peak for a phase transition such as solidification or the superfluid transition. Some state different to the semi-quantum liquid state is expected below 1.3 K. For further investigation of this problem, experiments at much lower temperatures are required.

### *3.3. He in ZSM-5 (three-dimensional system)*

Heat capacities have been observed for various concentrations of $^3$He and $^4$He adsorbed in ZSM-5 which has three-dimensional channels. The results for $^4$He are shown in figure 8($a$) for the lower-concentration region, and in figure 8($b$) for the higher-concentration region. Figure 9 shows the results for $^3$He. In these figures, the contribution of the atoms trapped on the surface is considered to be negligible, because the ratio of the number of atoms on the surface to the number adsorbed within the pores of ZSM-5 is about one-tenth of the ratio for ZSM-23. The present results are different to the heat capacities of liquid helium or solid helium. The heat capacities of both $^4$He and $^3$He have qualitatively the same dependence on temperature and concentration; we cannot distinguish between the Bose and Fermi system in these figures.

We now discuss the temperature dependence of the heat capacity taking into consideration the atomic concentration.

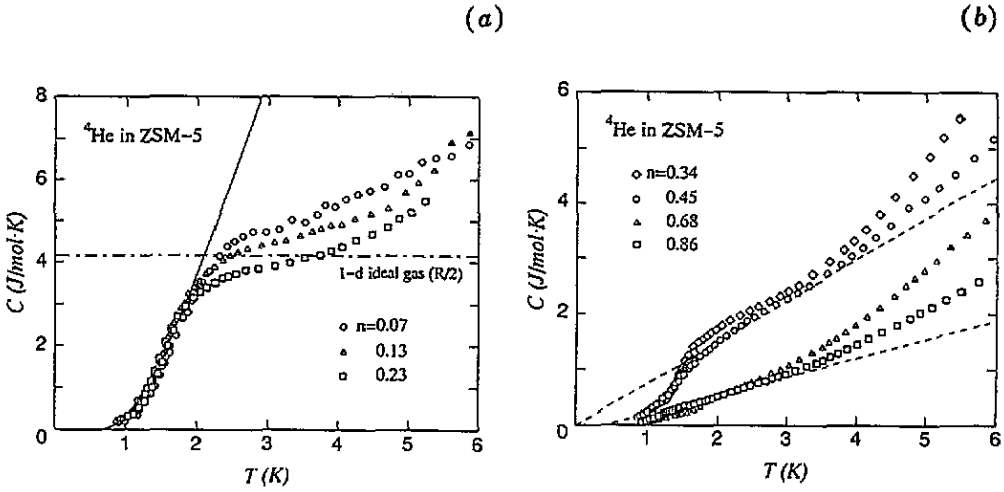


**Figure 8.** Heat capacities of $^4$He in ZSM-5. ($a$) Low-concentration region: $n = 0.07$ (○), 0.13 (△) and 0.23 (□). The full curve shows the heat capacity calculated using the model for a free particle mentioned in the text. ($b$) High-concentration region: $n = 0.34$ (◇), 0.45 (○), 0.68 (△) and 0.86 (□). The broken lines are to guide the eye.

First, the heat capacities of $^4$He and $^3$He for the low-concentration region ($n \lesssim 0.3$) increase abruptly with increasing temperature up to about 2 K as in figures 8($a$) and 9, respectively. It should be noted that in this temperature region the absolute values of the respective heat capacities of $^4$He and $^3$He merge on the respective common curve. The characteristic shoulder appears around 2 K. Above 2 K, heat capacities deviate from the common curve depending on the concentration.

As shown in figure 8($b$), the heat capacities of $^4$He for the high-concentration region decrease with increasing concentration. In this concentration region, the heat

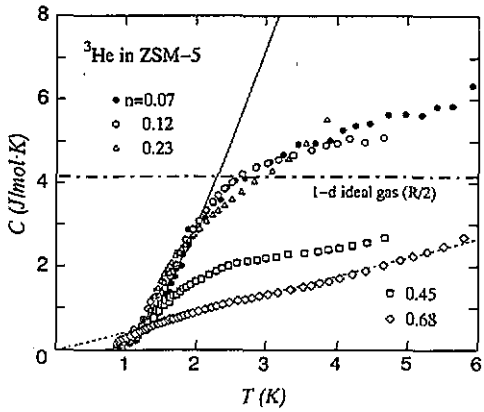


**Figure 9.** Heat capacities of $^3$He in ZSM-5. $n = 0.07$ (•), 0.12 (○), 0.23 (△), 0.45 (□) and 0.68 (◇). The full curve shows the heat capacity calculated using the model of a free particle mentioned in the text. The broken lines are to guide the eye.

capacity does not exhibit the clear shoulder observed around 2 K, and seems to give a linear dependence on temperature for $n \gtrsim 0.45$. The same thermal behaviour can be seen in the case of $^3$He, as shown in figure 9.

Before we discuss the absolute value of the heat capacity, a few remarks should be made concerning the possible position of a helium atom in the narrow channels of ZSM-5. A pore of ZSM-5 can be approximated as consisting of two parts: channel and cage. The cage, which is the space of intersection of zigzag and straight channels as shown in figure 1(*b*), is slightly larger than the channel itself. When a particle is confined in a narrow space, the kinetic energy of the particle increases due to quantum effects. The relation between the confined space size, $\Delta x$, and the increase of momentum, $\Delta p$, is given roughly by $\Delta x \Delta p \gtrsim \hbar$. Thus the increase in kinetic energy, $\Delta E$, is roughly

$$\Delta E \approx \frac{\Delta p^2}{2m} \gtrsim \frac{1}{2m}\left(\frac{\hbar}{\Delta x}\right)^2. \tag{6}$$

Substituting the mass of the $^4$He atom in (6), $\Delta E/k_B$ is nearly equal to 60 K for $\Delta x = 2$ Å, and 9.5 K for $\Delta x = 5$ Å, which respectively correspond to the effective size of the channel and the cage in ZSM-5, as will be mentioned below. This implies that the helium atom is more likely to exist in the cage than in the channel, for low concentrations at low temperatures.

We will now estimate the energy levels of a helium atom in the cage, assuming that the atom behaves as a free particle. The real space of the cage is too complex to let us calculate the energy levels. However, if we suppose that the cage is a small cube with side $\Delta x$, we can calculate the energy levels $E_n$ of the free particle as

$$E_n = \frac{\pi^2}{2m}\left(\frac{\hbar}{\Delta x}\right)^2 (n_x^2 + n_y^2 + n_z^2) \tag{7}$$

where $m$ is the mass of the particle and $n_i (i = x, y, z)$ are arbitrary natural numbers. The energy levels depend upon the cube size $\Delta x$ and mass $m$. The heat capacity

calculated by this model fits well the observed data for $^4$He with $m = 4$ amu and $\Delta x \simeq 5$ Å in the low-concentration region ($n \lesssim 0.3$) below 2 K, and for $^3$He with $m = 3$ amu and $\Delta x \simeq 5.2$ Å (see the full curves in figures 8($a$) and 9). Since the difference among energy levels in $^3$He is larger and more discrete than in $^4$He, the heat capacity of $^3$He is smaller than that of $^4$He at the same temperature.

This model is somewhat oversimplified. However, it suggests that helium atoms adsorbed in ZSM-5 have enhanced discrete energy levels in the restricted space of the pore at temperatures below 2 K.

We now consider the effective size, $\Delta x$, of the cage mentioned above. It has been reported that the cage can contain at most about eight nitrogen molecules [17]. The cage must therefore have a space of at least 8 Å to contain eight nitrogen molecules. If we take the diameter of the He atom to be of the order of 3 Å, an effective value of $\Delta x \simeq 5$ Å may be reasonable. In other words, more than eight helium atoms (in fact, about 11) are contained in the cage. The experiment shows that helium atoms behave as free particles until the atomic concentration comes to $n \simeq 0.3$, which corresponds to three atoms per cage. In other words, when a cage includes more than three atoms, each atom becomes affected by interatomic interactions and cannot behave like a free particle.

Turning back to the experimental results above 2 K, in figure 8($a$) we can see something like a plateau in the heat capacity, which gives a value of about $R/2$ for low $^4$He concentrations. This implies that $^4$He atoms go through freely in the one-dimensional or zigzag channels leaving the cage. For temperatures higher than 4 K, the heat capacity increases rather steeply. This is considered to be due to the possible degassing effect at higher temperatures. In the case of the heat capacity of $^3$He, for the corresponding concentration, there seems to be a trace of the same plateau around 3 K, as in figure 9.

On the other hand, in the heat capacity for the higher-concentration region ($n \gtrsim 0.3$) the characteristic shoulder around 2 K disappears, and it comes to depend linearly on temperature with increasing concentration (figure 8($b$)). This temperature dependence of the heat capacity looks similar to the case of helium atoms adsorbed in the one-dimensional channel (ZSM-23). In this concentration range, helium atoms are supposed to be so close to each other as to behave like a semi-quantum liquid in the three-dimensional channels. The coefficient of the linear term $A(n)$ for the present case is of the same order as that for the one-dimensional channel (ZSM-23). This is relevant to the comparable size of pore between ZSM-23 and ZSM-5.

## 4. Conclusion

In this study, the thermal behaviour and the quantum effects of $^4$He and $^3$He in a severely restricted geometry have been investigated. The heat capacities of helium atoms in the one- and three-dimensional channels of high-silica zeolites have been observed below 6 K. The results are concluded as follows.

(i) In one-dimensional channels in ZSM-23 the heat capacity depends linearly on temperature as $C = A(n)T$. The coefficient $A(n)$ decreases monotonically as the concentration increases. This result can be interpreted by the semi-quantum liquid model on the basis of a tunnelling two-level system, whose mechanism has been introduced to explain the thermal behaviour of glasses or amorphous solids at very low temperatures. We have found that the coefficient $A(n)$ of the present

result is much larger than that in glasses, and the temperature range where the heat capacity keeps the linear dependence is much wider for helium than for glasses. These are responsible for the larger zero-point motion of helium. Although the linear dependence is observed for helium atoms under pressure, or in a space where the direct positional exchange of atoms is possible, the present work has revealed, for the first time, that the linear dependence is realized for a one-dimensional system in which positional exchange is prohibited.

(ii) In the three-dimensional system in ZSM-5, which is structurally approximated to consist of channels and cages, the observed heat capacity for the lower helium concentration $n \lesssim 0.3$ shows a characteristic hump around 2 K. The results below 2 K are reproduced by a consideration of the discrete energy levels of helium enhanced in the cage. For higher concentrations, the heat capacity comes to show the linear dependence on temperature, and can no longer be explained by the above model. This temperature dependence can be understood using the same picture of a semi-quantum liquid as in the case of ZSM-23.

(iii) Quantum degeneracy, such as the superfluidity of $^4$He and the Fermi degeneracy of $^3$He, is expected for $^4$He (boson) and $^3$He (fermion) but does not occur in the present restricted geometry. Concerning this problem, it is pointed out that quantum degeneracy is suggested, both theoretically [10–12] and experimentally [13], to occur in three-dimensional systems. It is also suggested, by Giamarchi and Schulz [26], that a superfluid transition of a one-dimensional boson gas may be possible. Our results do not completely deny the possibility of quantum degeneracy in the restricted geometries at lower temperatures.

In order to make clear the contrast in thermal behaviour of the quantum effect of helium in the present system, we are presently investigating the heat capacity of classical particles, e.g. neon, in the same zeolites. It is expected that neon atoms adsorbed in high-silica zeolites show something like solidification at low temperatures because of the larger van der Waals interactions. Our preliminary results are mostly explained by the successful models of solids, the Debye model and the Einstein model, giving a distinct difference from the case of helium. More detailed data concerning neon adsorbed in high-silica zeolites will be published elsewhere.

## Acknowledgments

The authors would like to express sincere thanks to Dr O Terasaki of Tohoku University and Dr S Ueda of Osaka University for supplying the high-silica zeolite samples. They are grateful to Professor T Haseda for his constant interest and valuable comments.

## References

[1] Tait R H and Reppy J D 1979 *Phys. Rev.* B **20** 997
[2] Bishop D J and Reppy J D 1980 *Phys. Rev.* B **22** 5171
[3] Brewer D F and Rolt J S 1972 *Phys. Rev. Lett.* **27** 1485
[4] Shirahama K, Kubota M, Ogawa S, Wada N and Watanabe T 1990 *Phys. Rev. Lett.* **64** 1541
[5] Bretz M, Dash J G, Hickernell D C, McLean E O and Vilches O E 1973 *Phys. Rev.* A **8** 1589
[6] Wada N, Ito T and Watanabe T 1984 *J. Phys. Soc. Japan* **53** 913
[7] Kato H, Wada N, Ito T, Takayanagi S and Watanabe T 1986 *J. Phys. Soc. Japan* **55** 246

[8] Wada N, Yamamoto Y, Kato H, Ito T and Watanabe T 1986 *Proc. 7th Int. Zeolite Conf. (Tokyo 1986)*
[9] Kato H, Ishioh K, Wada N, Ito T and Watanabe T 1987 *J. Low Temp. Phys.* **68** 321
[10] Minoguchi T and Nagaoka Y 1987 *Prog. Theor. Phys.* **78** 552
[11] Sano K, Doi I and Minoguchi T 1987 *J. Phys. Soc. Japan* **56** 1920
[12] Doi I 1989 *J. Phys. Soc. Japan* **58** 1312
[13] Deguchi H, Moriyasu Y, Amaya K, Kitaoka Y, Kohori Y, Terasaki O and Haseda T 1987 *Japan. J. Appl. Phys.* **26** 311 suppl **26-3**
[14] Wright P A, Thomas J M, Millward G R, Ramdas S and Barri S A 1985 *Chem. Commun.* 1117
[15] Kokotailo G T, Lawton S L, Olson D H and Meier W M 1978 *Nature* **272** 437
[16] Flanigen E M, Bennett J M, Grose R W, Cohen J P, Patton R L, Kirchner R M and Smith J V 1978 *Nature* **271** 512
[17] Jacobs P A, Beyer H K and Valyon J 1981 *Zeolites* **1** 161
[18] Roy N N and Halsey G D 1971 *J. Low Temp. Phys.* **4** 231
[19] Andreev A F 1978 *Sov. Phys.-JETP Lett.* **28** 556
[20] Harada J and Ohshima K 1981 *Surf. Sci.* **106** 51
[21] Anderson P W, Halperin B I and Varma C M 1972 *Phil. Mag.* **25** 1
[22] Phillips W A 1972 *J. Low Temp. Phys.* **7** 351
[23] Zeller R C and Pohl R O 1971 *Phys. Rev.* B **4** 2029
[24] Everett D H and Powl J C 1976 *Faraday Trans.* I **25** 59
[25] Miyagi H, Haseda T and Nakamura T 1985 *J. Phys. Soc. Japan* **54** 1299
[26] Giamarchi T and Schulz H J 1987 *Europhys. Lett.* **3** 1287